ITER Limiters Moveable during Plasma Discharge and Optimization of Ferromagnetic Inserts to Minimize Toroidal Field Ripple

K. Ioki 1), V. Chuyanov 1), F. Elio 1), D.Garkusha 2), Y. Gribov 1), E.Lamzin 2),
M. Morimoto 1), M. Shimada 1), M. Sugihara 1), A. Terasawa 1), Yu Utin1), X. Wang 1),

1) ITER International Team, Boltzmannstr. 2, 85748 Garching, Germany
2) "Sintez", Efremov Inst., 189631 Metallostroy, St. Petersburg, Russia

e-mail contact of main author: Kimihiro.Ioki@iter.org

Abstract. --- In a new startup/shutdown limiter concept, the limiters are retracted by ~80 mm during the plasma flat top phase. This concept gives important advantages; the particle and heat loads due to disruptions, ELMs and blobs on the limiters will be mitigated approximately by a factor 1.5 or more; the coupling of the ICRH power will be improved. A flexible support of thin plates is used for the limiter system and there is no sliding support inside the vacuum, to keep the reliability of the system. Driving mechanisms are located outside the vacuum boundary. The ferromagnetic inserts have previously not been planned to be installed in the midplane region. It causes a relatively large ripple (~1 %) in a limited region of the plasma and the toroidal field flux line fluctuation ~10 mm. It is shown that additional ferromagnetic inserts between equatorial ports reduce the ripple and the flux fluctuation significantly.

1. Introduction

Two important design updates have been made in the ITER vacuum vessel (VV) and in-vessel components recently. One is the introduction of limiters moveable during a plasma discharge, and the other is optimization of the ferromagnetic insert configuration.

2. Limiters Moveable during Plasma Discharge

The ITER start-up/shutdown limiters will be installed in equatorial ports at two toroidal locations. The two port limiters (PL) must be aligned very accurately based on the magnetic flux lines. The relative difference of the two limiter positions should be within ~2 mm according to a recent analysis. Otherwise, the heat load on one of the two limiters becomes very high. Therefore, an alignment system is required for the limiter to fix the limiter FW surface very accurately in relation to the magnetic flux lines [1]. This alignment system was designed for use between plasma shots (not during plasma burn). As shown in Fig.1, the port limiter structure was designed with an alignment system using eccentric rotating mechanisms. The required range and accuracy of the adjustments are summarized in Table 1.

The limiter plasma-facing surface protrudes ~80 mm from the blanket first wall (FW) during the start-up and shutdown phase. However, the limiter should not necessarily protrude during the divertor configuration phase. In the new limiter concept which has been developed recently for ITER, the limiters are retracted by ~80 mm during the plasma flat top phase. This concept gives important advantages:

(i) the gap between the plasma and the ICRH antenna can be reduced to improve the coupling of the ICRH power, with the ICRH antenna in a protected position flush with the blanket FW.

(ii) the particle and heat loads due to disruptions, ELMs and blobs on the limiters will be mitigated.

The maximum distance of the movement is typically 80mm, and the time scale of the movement is 5s. A self-braking worm gear jack system is proposed as the moving and locking mechanism. This scheme releases the constraint on the cumulative plasma distance, bringing it 40 mm closer to the ICRH antenna (better coupling expected), without increasing the ELM/disruption heat loads on the limiter FW. An improved Alignment System (AS) retracts the PL after the start, to keep it flush with the primary FW during the pulse and to deploy it quickly for plasma termination, anytime it is requested.

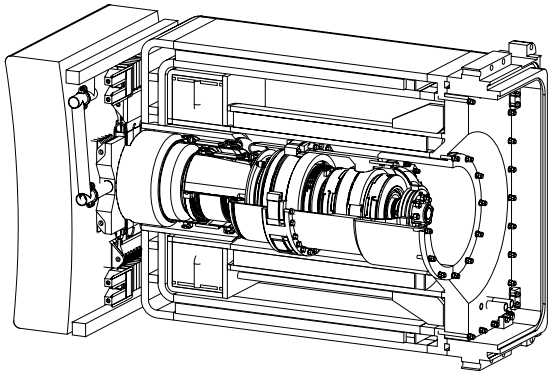

Fig. 1 2001 Limiter design

Table 1 Requirements of alignment system

	Required range for adjustment	Required accuracy of adjustment
Radial movement	±20 mm	±0.5 mm
Rotation (tilt) around the horizontal axis*	±0.546°	10%
Rotation (tilt) around the vertical axis*	±0.695°	10%

*Both max. rotations correspond to the radial forwarding/retraction of the corner points ±10 mm.

The engineering design has progressed taking into account electromagnetic loads during plasma disruptions and VDEs. Considering very tight alignment requirements, the limiter position and angles can be precisely adjusted between plasma shots and after the adjustment they are locked. Keeping this precise alignment when protruding, the limiter can be moved back and forth in the radial direction during a plasma discharge. A schematic view of the new limiter system is shown in Fig.2. A flexible support of thin plates is used and there is no sliding support inside the vacuum, to keep the reliability of the system. Driving mechanisms are also located outside the vacuum boundary. Comparing with the previous design (shown in Fig. 1), the supporting and alignment structure is simplified and high reliability is expected.

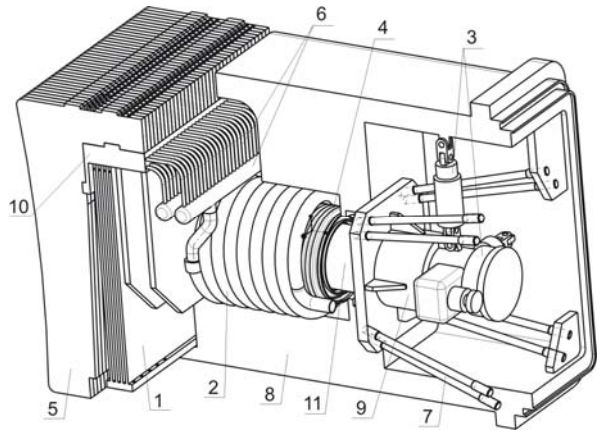

1: Flexible support of thin plates
2: Inlet and outlet pipes (helical)
3: Driving mechanism (motor)
4. Bellows (vacuum boundary)
5: Sliced limiter plates
6: Cooling pipes and headers
7: Flexible support rods
8: Housing (nuclear shielding)
9: Central shaft
10: Upper base plate
11: Central shaft

Fig.2 Limiter system moveable during plasma discharge

Basic design features of the new design are summarized as follows,

(a) Flexible supports to avoid jamming (no sliding in vacuum). Calculation results for the peak heat flux on the limiter during start-up and normal operation.

(b) Flexible helical pipes without bellows in the water boundary.

(c) External drive and screw jacks accessible for maintenance.

(d) Long bellow for vacuum seal.

(e) Limiter plates with individual attachment and hydraulic connections (see Fig. 3).

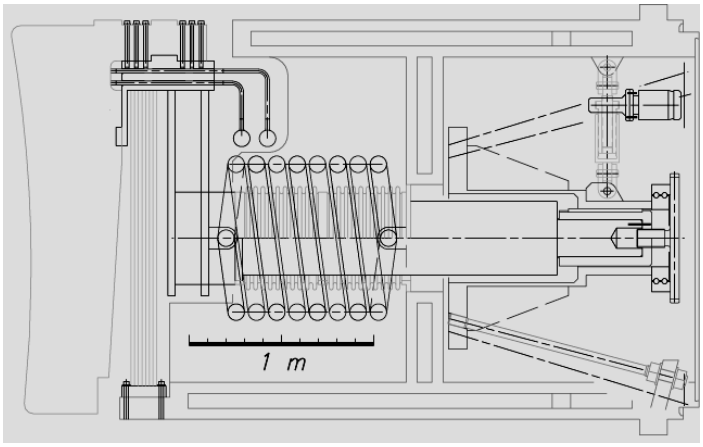

Fig. 3 Elevation view of moveable port limiter

It is expected that the coupling of the ICRH power will be improved by a factor of 1.5-2 when the gap between the plasma and the ICRH antenna is reduced by 2-4 cm (see Fig. 4). In addition, the FW location was updated to follow the plasma boundary shape in the outboard midplane region, which also improves the ICRH power coupling.

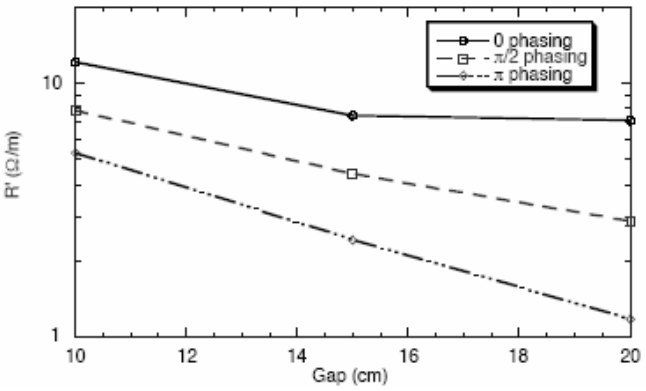

Fig. 4 ICRH power coupling versus gap between plasma and antenna

It is calculated that the peak heat load on the limiter during the start-up phase is 4.7 MW/m^2 in the reference case, and this value will be decreased when the divertor configuration starts at a lower plasma current. (Table 2).

Table 2 Heat flux on the limiter (reference case)

Peak heat flux at the limiter during start-up (MW/m^2)	4.7
Maximum heat flux at the limiter during flat-top (MW/m^2)	0.5

The heat loads during ELMs and disruption thermal quench are estimated as shown in Fig. 5 and 6 [2], [3]. According to the estimation, the thermal quench energy load is more severe and may produce melting on the beryllium surface depending on the condition. The thermal quench energy load parallel to the field line on an arbitrary point x of the limiter can be expressed by the equation: $\frac{28.6E_{disr}}{\lambda}e^{-(\frac{L_0+x}{\lambda})}$, where E_{disr} is the total energy loss during disruption (MJ), L_0 is the distance between the separatrix and limiter head (mm), x is the distance from limiter head (mm), $\lambda=fe\times\lambda ss$, λss is the steady state heat flux width = 5 mm, and fe is the expansion factor during disruption (5 or 10).

The heat loads are reduced by approximately a factor of 1.5 when the limiter is retracted as summarized in Table 3. The erosion rate due to the thermal loads and particle flux will also be reduced.

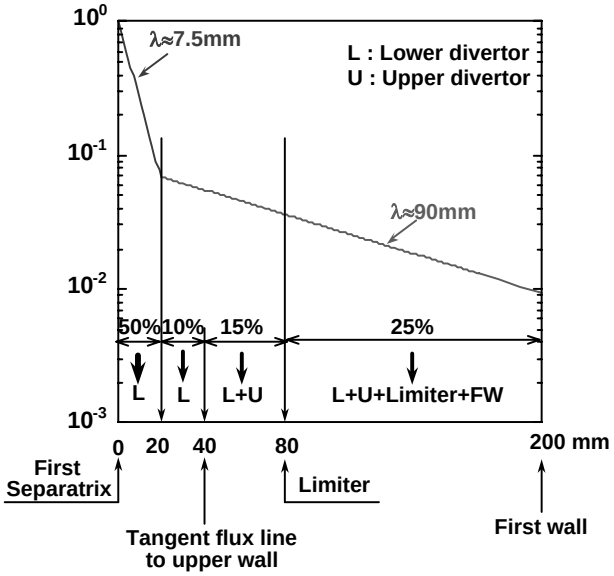

Fig. 5 Estimated ELM heat load (extrapolated from [4])

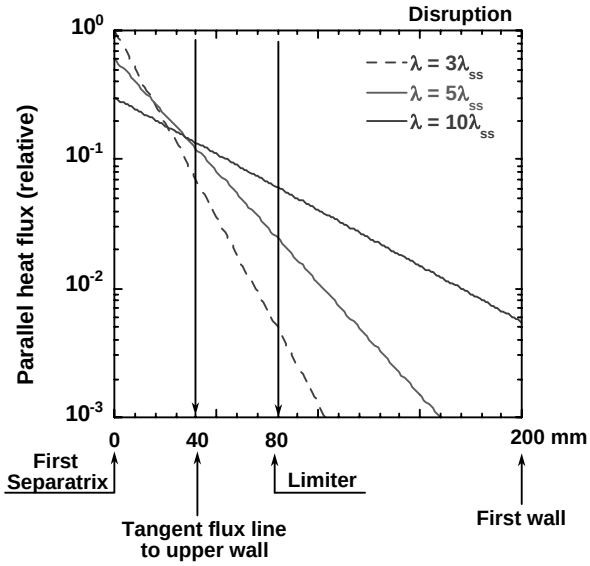

Fig. 6 Estimated heat load during disruption thermal quench (derived from [5])

Table 3 Peak heat load on the limiter during ELMs and disruption thermal quench

ELM Energy Loss	3 MJ	15MJ
Peak heat load - protruded	0.06 MJ/m^2	0.3 MJ/m^2
Peak heat load - retracted	0.04 MJ/m^2	0.2 MJ/m^2

Disruption thermal quench Energy Loss	175MJ	350MJ
Peak heat load - protruded	0.8-6* MJ/m^2	1.5-12* MJ/m^2
Peak heat load - retracted	0.4-3.9* MJ/m^2	0.8-7.9* MJ/m^2

*Range corresponds to the decay length of $5\lambda_{ss}$ (25 mm) and $10\lambda_{ss}$ (50 mm) at the outer midplane.

3. Optimization of Ferromagnetic Inserts to Minimize Toroidal Field Ripple

(1) Functions and structure of in-wall shielding

The ITER in-wall shielding is installed between the double walls of the ITER VV. Approximately 60 % of inter-shell space is filled with in-wall shielding [6]. The in-wall shielding has two main functions. One is nuclear shielding and the other is reduction of the toroidal field ripple. The in-wall shielding dedicated to the former function is called “primary in-wall shielding”. The primary in-wall shielding material is boron-doped stainless steel (boron content; 1-2 wt %). The in-wall shielding used for both nuclear shielding and ripple reduction is called “ferromagnetic insert”.

The in-wall shielding is designed to reduce induced current and subsequent electromagnetic forces on shield blocks. All large electrical circuits in the structure, which may cause significant electromagnetic forces, have been avoided or carefully arranged to minimize them. The in-wall shielding is suitably segmented into blocks considering handling during the assembly and limiting induced eddy current during operation. The shield block is supported by poloidal ribs or localized poloidal ribs that connect two blanket flexible support

housings so that the total toroidal electrical resistance is sufficient to limit the induced current while allowing magnetic field penetration. A gap is maintained between the two adjacent blocks to provide the electrical isolation, even taking into account dimensional tolerances. With this configuration, the toroidal resistance of the VV including the in-wall shielding is ~ 7.9 μΩ, which results in the overall toroidal resistance higher than the required value ~ 7 μΩ.

The shield block consists of 3~11 stacked flat plates whose thicknesses are all 40 mm. The plates are bolted together to form a shield block as shown in Fig.7. The innermost plate of a shield block (i.e., the plate closest to the inner shell) is supported by a bracket attached to the poloidal rib. The outer face of the shield block will be fixed by bolts to the rib using another bracket. The two brackets are at the same poloidal location so that the poloidal electrical resistance of the vessel is not reduced even by including shield blocks.

(2) Ferromagnetic inserts

The ferromagnetic inserts are installed in the plane of the TF coil in the outboard area from 12 to 5 o'clock region in the poloidal cross section. The location and the filling factor of the ferromagnetic inserts have been optimized based on the field ripple calculation. SS 430 has been selected because of its high mechanical strength, good machinability, and corrosion resistance. It has a saturated magnetization of approximately 1.5 T. The filling factor is adjusted by selecting ferromagnetic steel plates among the plates in each shield block. The ferromagnetic inserts are located periodically in the toroidal direction.

Electromagnetic analyses have been performed to evaluate electromagnetic forces on the ferromagnetic insert due to magnetization in the external magnetic fields, which is expected to be the major load on the ferromagnetic insert. A 3-D electromagnetic analysis has been performed using a 20 degree toroidal angle model with solid elements. Cyclic boundary conditions have been applied to simulate full torus. TF coils, CS coils, PF coils and plasma have been defined by numerical data modelling steady state operation. The D-shape of the TF coil is modelled considering the local magnetic field near the ferromagnetic insert. The current in a TF coil is 9.1 MAturn/coil corresponding to B_t = 5.3 T at R = 6.3 m. The modelled operation is scenario 2 and the plasma current is 15 MA in steady state. The calculated maximum electromagnetic forces due to magnetization acting on a ferromagnetic insert block are 18.2 kN in the poloidal direction and 7.1 kN in the outward direction normal to the block surface (see Fig. 8). These values are forces for a ferromagnetic shield block at a 2.5 degree toroidal angle.

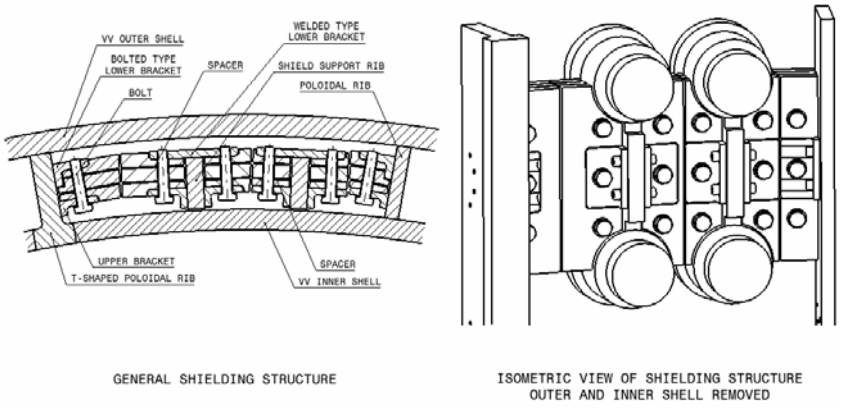

Fig. 7 Structure of in-wall shielding

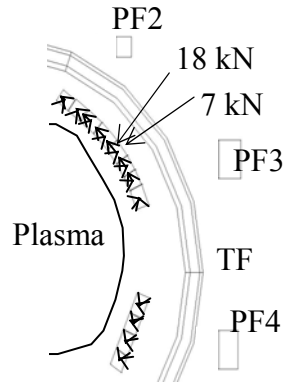

Fig. 8 EM forces on ferromagnetic inserts

(3) Additional ferromagnetic inserts

The ferromagnetic insert was previously not installed in the outboard midplane region between equatorial ports due to irregularity caused by the tangential ports for neutral beam injection. As shown in Fig.8, the available space for the ferromagnetic insert is quite different and limited between the regular port area and the NB port area. The lack of the ferromagnetic inserts in the midplane causes a relatively large ripple (~1 %) in a limited region of the plasma (see Fig. 9), which nevertheless seems acceptable from the plasma performance viewpoint. However, toroidal field flux lines fluctuate ~10 mm due to the large ripple in the FW region. To avoid problems due to the TF flux line fluctuation, the possibility of installing ferromagnetic inserts in the equatorial port region has been studied. It is difficult to achieve the same configuration of the additional ferromagnetic insert in each toroidal location due to the constraint of the supporting structure of the shield blocks. Therefore, the same volume of ferromagnetic insert is added in every sector but with different shapes between regular sectors and NBI sectors. As shown in Fig. 10, the volume of the additional ferromagnetic insert is adjusted to make the magnetic configuration toroidally cyclic as much as possible to minimize the effect of lower mode error fields. The toroidal field ripple in the outermost midplane plasma region and the magnetic flux line deviation in the midplane FW region have been calculated as a function of the filling factor of the additional ferromagnetic insert. The ripple distribution (with the filling factor 50 % of the additional ferromagnetic insert) is shown in Fig. 11. The ripple and the magnetic flux deviation are linearly reduced with increasing filling factor as shown in Fig. 12. The filling factor 50 % gives the ripple ~0.3 % and the flux deviation ~3 mm. It is shown that the additional ferromagnetic insert effectively reduces the maximum ripple at the TF full current. On the other hand, the ripple is overcompensated (approximately -0.7 %) and the flux line deviation is 5 mm with the filling factor 50 % at the half TF current operation (see Fig. 12).

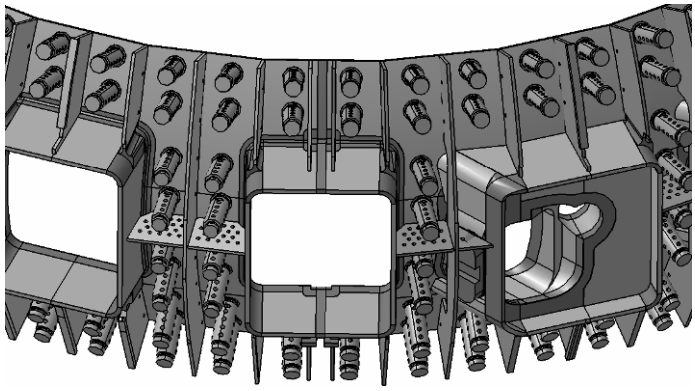

Fig. 8 VV inter-space layout in equatorial port region

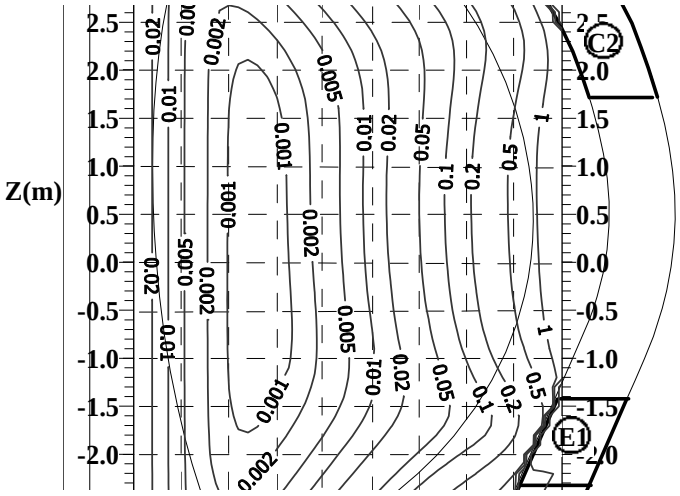

Fig. 9 Toroidal field ripple without additional ferromagnetic insets (Full TF current)

There is a concern that there will be a lower-mode error field due to the ferromagnetic insert layout not exactly cyclic in the mid-plane region because the configurations of the

ferromagnetic inserts in the NB region and the regular region are slightly different. However, the effect of the difference will be smaller than that of the test blanket modules (TBM) where the amount of the ferromagnetic material for the TBM is ~3.2 tonnes per port. The effects of both the ferromagnetic materials are being analyzed to see what additional ripple they add and this will be reported in the future.

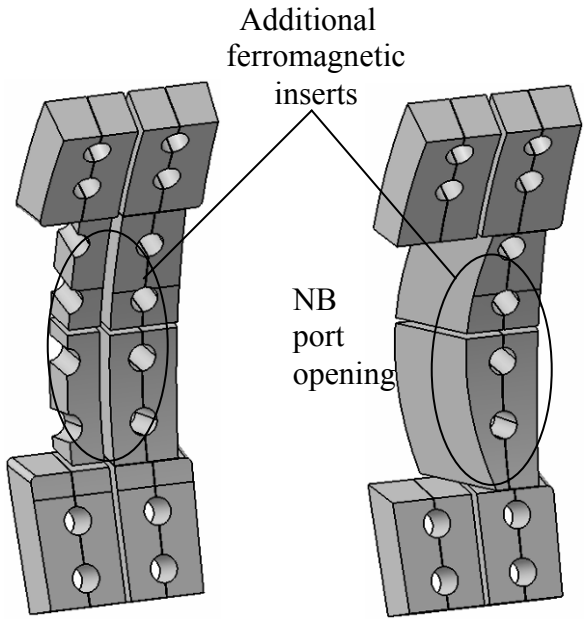

(Regular port region) (NB port region)
Fig. 10 Additional ferromagnetic inserts between equatorial ports

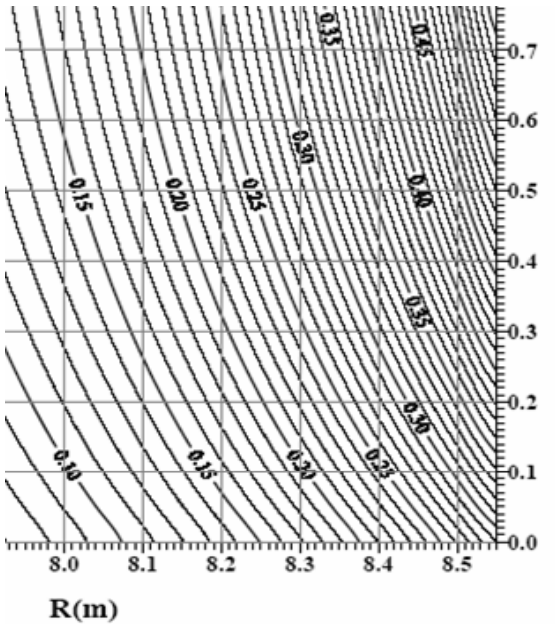

Fig. 11 Toroidal field ripple with additional ferromagnetic insets (50% filling factor) (Full TF current)

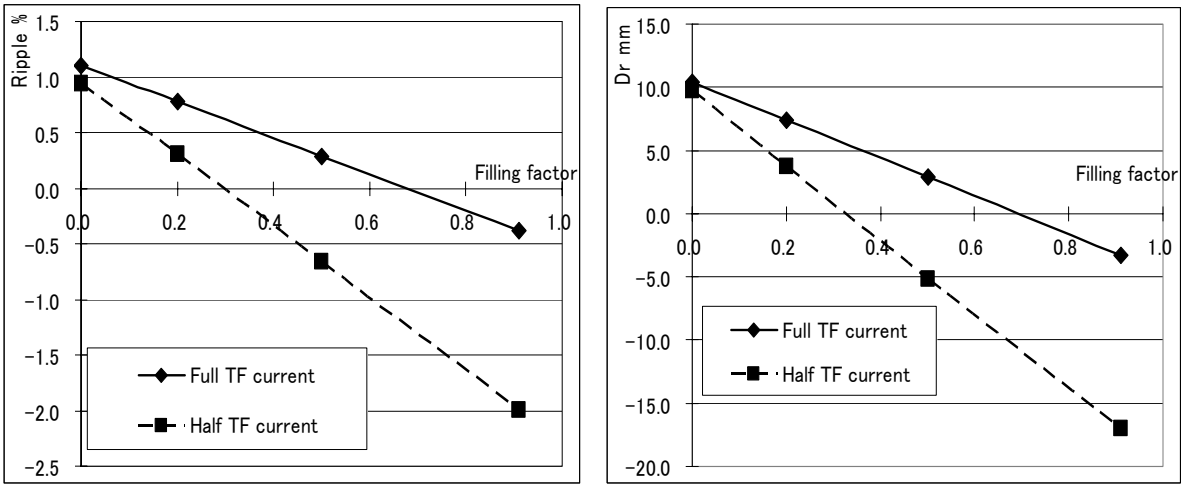

Fig. 12 The toroidal field ripple and the field line deviation as a function of the filling factor of the additional ferromagnetic insert (R=8.28m, Z=0.6m)

4. Conclusions

There have been a few design updates in the ITER vacuum vessel and in-vessel components recently. Two important ones are highlighted in this paper. One is limiters moveable during a plasma discharge, and the other is further optimization of the ferromagnetic insert configuration.

In the new limiter concept, the limiters are retracted by ~80 mm during the plasma flat top phase. This concept gives advantages: (a) the coupling of the ICRH power is improved by reducing the gap between the plasma and the ICRH antenna, with the ICRH antenna in a protected position flush with the blanket FW, (b) the particle and heat loads due to disruptions, ELMs and blobs on the limiters will be mitigated. At the same time, the limiter structure including the alignment system has been simplified and high reliability is maintained avoiding a sliding mechanism in the vacuum. Elements where maintenance is expected (such as electrical connections, motors, screws) are accessible from the outside.

Considering irregularity caused by the tangential ports for neutral beam injection, it was not planned to install ferromagnetic inserts in the outboard midplane region. Their absence causes a relatively large ripple (~1 %) and a toroidal field flux line fluctuation of ~10 mm. When additional ferromagnetic inserts are installed in the equatorial port region to mitigate problems due to the TF flux line fluctuation, they effectively reduce the maximum ripple and the TF flux fluctuation.

Acknowledgements

This report was prepared as an account of work undertaken within the framework of ITER Transitional Arrangements (ITA). These are conducted by the Participants: the European Atomic Energy Community, Japan, India, the People's Republic of China, the Republic of Korea, the Russian Federation, and the United States of America, under the auspices of the International Atomic Energy Agency. The views and opinions expressed herein do not necessarily reflect those of the Participants to the ITA, the IAEA or any agency thereof. Dissemination of the information in this paper is governed by the applicable terms of the former ITER EDA Agreement.

References

[1] A. Cardella et al., "Design and manufacturing of the ITER limiter", Fusion Engineering and Design 61-62 (2002) 111-116.
[2] M. Sugihara "Energy load and flux on various parts during phases of plasma start-up, normal operation, ELMs and disruptions" ITER_D_22F99Z v1.0.
[3] M. Sugihara "Energy load on first wall/limiter due to the thermal quench during disruptions - with including the effect of plasma movement " ITER_D_22M5D5 v1.0.
[4] A. Herrmann et al., PPCF 46 (2004) 971.
[5] A. Loarte et al., 20th IEAE FEC, Vilamoura, Portugal, IAEA-CN-116/IT/P3-34 (2004).
[6] K. Ioki et al., "Design and material selection for ITER first wall/blanket, divertor and vacuum vessel", Journal of Nuclear Materials 258-263 (1998) 74-84.